INTERNATIONAL JOURNAL OF AUTOMOTIVE AND MECHANICAL ENGINEERING (IJAME)
ISSN: 2229-8649 e-ISSN: 2180-1606
VOL. 20, ISSUE 1, 2023, 10274 – 10284
DOI: https://doi.org/10.15282/ijame.20.1.2023.09.0794

ORIGINAL ARTICLE

# Parametric Analysis of a Divided Rocker for Battery Electric Vehicles

Haseeb Shafaqat[1,*], Christopher Krüger[2] and Peter Urban[2]

[1]Department of Mechanical and Automotive Engineering, Sirindhorn International Thai-German Graduate School of Engineering, King Mongkut's University of Technology North Bangkok, 10800 Bangkok, Thailand
[2]Institute for Automotive Engineering (ika), Faculty of Mechanical Engineering, RWTH Aachen University, 52062 Germany

**ABSTRACT** – The driving range of an electric vehicle can be increased through an efficient integration of the large battery within the vehicle structure. In this regard, a divided rocker concept from an existing study is investigated, in which the vehicle rocker is divided into two parts by means of a division plane. One part of the rocker remains vehicle sided and enables the attachment of the surrounding vehicle structures, while the other part is functionally integrated into the side frame of the battery housing. In the scope of this paper, several division plane concepts for such a divided rocker are created and analyzed. The crash performance of the modelled division plane concepts is studied on a component level using the side pole crash test as a load case. For the different division planes, a parametric analysis is performed by varying the number of chambers in the rocker profile, the chamber width, mass distribution, individual section thicknesses, the height of the division planes, and the air gap between the vertical surfaces of the division planes. Several crash performance criteria, such as structural deformation, force, and energy absorption, are examined. Among the studied parameters, the number of chambers and mass distribution have notable influences, while individual section thicknesses and the height of the division planes do not have a significant influence on the crash performance. Lastly, stiffer chambers in the battery-sided rocker created by decreasing the chamber width have the strongest effect on crash performance.

**ARTICLE HISTORY**
Received: 13th July 2022
Revised: 24th Nov. 2022
Accepted: 02nd March 2023
Published: 03rd Apr 2023

**KEYWORDS**
*Electric vehicles;*
*Battery housing;*
*Vehicle rocker;*
*Crash test;*
*Crash performance*

## INTRODUCTION

Amid growing concerns about climate change and rising global temperature, governments and regulatory bodies are introducing laws and policies to reduce $CO_2$ emissions and shift towards renewable energy sources. In this regard, the European Union has put forward a plan to cut $CO_2$ emissions by at least 55% below 1990 levels by 2030 [1]. The United States government has also set a target for reaching net-zero greenhouse gas emissions by 2050 [2]. To meet tighter emission restrictions and targets set by governments, automotive manufacturers are focusing on battery electric vehicles, among other alternatives [3]. As the driving range is one of the major customer concerns regarding Battery Electric Vehicles (BEVs), large batteries are integrated within the vehicle structure to achieve a similar driving range as conventional Internal Combustion Engine (ICE) vehicles [4]. The battery of modern electric vehicles is located below the vehicle floor, as indicated in Table 1.

**Table 1.** Overview of recent electric vehicle batteries [7], [8]

| Car Model | Battery (*kWh*) | Cell Type | Location |
|---|---|---|---|
| VW I.D.4 | 82.0 | Pouch | Floor |
| Ford Mustang Mach-E | 98.7 | Pouch | Floor |
| Hyundai Ioniq 5 | 72.6 | Pouch | Floor |
| Tesla Model S | 95.0 | Cylindrical | Floor |
| Mercedes-Benz EQS | 120.0 | Pouch | Floor |
| Porsche Taycan | 93.4 | Pouch | Floor |
| BMW iX | 111.5 | Prismatic | Floor |
| Polestar 2 | 78.0 | Pouch | Floor |
| Audi Q4 e-tron | 82.0 | Pouch | Floor |

The benefits of the battery location within the area of the vehicle floor include increased torsional stiffness for the vehicle body and low centre-of-gravity of the vehicle. However, the placement of the battery below the vehicle floor poses a challenge regarding crash safety [5]. Incidents of fire during and after a crash and recalls of electric vehicles by manufacturers over battery fire concerns indicate the need for the safe integration of the battery within the vehicle

*CORRESPONDING AUTHOR | Haseeb Shafaqat | ✉ haseebshafaqat@gmail.com

structure [5]. A review study of battery fire incidents in electric vehicles highlights the need for reducing deformations during side crash incidents [6].

To ensure the safety for a battery electric vehicle, several safety tests are conducted by regulatory bodies on a system level and on a full vehicle level. On a system level, a series of tests, such as UNECE R100 is performed on the battery system of electric vehicles [9], [10]. These tests include mechanical shock and integrity, vibration, fire resistance, short circuit protection, and over-temperature protection [11]. In order to pass these system-level tests, the battery cells typically need to be housed in a sealed enclosure that can protect these cells from external loads instead of integrating the individual battery cells or modules directly into the vehicle structure.

On a full vehicle level, frontal and side crash tests are performed, in which the vehicle collides with deformable or rigid barriers at high velocities [12]. A side pole crash is critical for the vehicle structure due to the limited available area between the occupant and the pole for absorbing crash energy and the concentrated application of force from the pole in a lateral direction [13]. Such a test, according to Euro NCAP, involves a vehicle colliding from the side at a 75° angle with a rigid pole at 32 km/h [12]. For electric vehicles where the battery is located within the area of the vehicle floor, the most critical crash scenario is a side pole crash test [14] since, in addition to the occupants, the battery cells located below the vehicle floor also need to be protected in a side crash scenario. Therefore, a key function of the battery housing and the vehicle rocker in electric vehicles is to withstand external loads and protect the battery cells in the event of a crash.

## AIM AND DESIGN METHODOLOGY

There is a need for space-efficient packaging of the large battery inside the vehicle structure that also conforms to crash safety regulations [15]. Several studies have explored the potential of optimized battery placement inside the vehicle structure, such as incorporating a battery housing with thermal functions [16], battery housing modification for reducing mass [17], and battery system packing efficiency analysis [15]. This paper is based on an existing study for a functionally integrated battery housing, in which a divided rocker concept was developed to reduce the structural redundancies between the vehicle body and the battery housing [18], [19]. In accordance with this study, as a requirement, the battery housing should be able to attach and detach from the vehicle body during assembly/disassembly and repairs. Moreover, since several safety tests are typically performed on the battery on a system level [9], [10], [11], it is beneficial to keep the structures of the battery housing as a separate system. Following the approach of [18], [19], for a space-efficient integration, the battery side frame is designed to be a part of the vehicle rocker. The concept divides the vehicle rocker into two parts while maintaining the outer dimensions of the vehicle rocker from the reference vehicle taken from the EU-funded project ALIVE [20]. This not only allows detachability of the battery housing but also avoids any major changes to the surrounding structure of the vehicle body where components such as A-pillar, B-pillar and seat cross members are connected.

In accordance with [19], the vehicle rocker is divided by means of a division plane and the upper part of the rocker is attached to the seat cross-members while the lower part is integrated into the side frame structure of the battery housing. A general division plane is shown in Figure 1. The aim of this study is to investigate the design possibilities for such a division plane concept on a component level. First, the boundary conditions for designing such a division plane are identified with the aim of creating division planes that are manufacturable and comparable to each other. A design analysis is then performed on the created variants in order to select more suitable division plane designs based on the defined requirements. The selected division plane concepts are then modelled and the crash behaviour is studied on a component level side pole crash test.

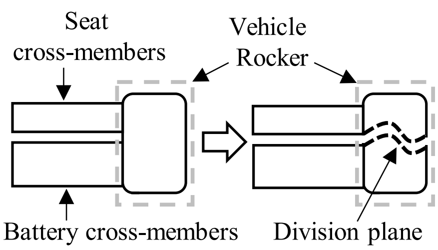


**Figure 1.** Divided vehicle rocker concept in accordance with [19]

A parametric analysis of the selected division planes is performed. The goal of the parametric analysis is to study the influence of the parameters on intrusion, force and energy absorption during a component-level side pole crash test. The study aims to identify the most influential parameters regarding the crash performance of such a divided rocker concept that can result in a lightweight design with a better crash performance.

### Conceptual Design

Since the divided rocker consists of two parts, it needs to fulfil the individual functional requirements of the associated structures. When joined together, the divided rocker must also perform the combined functions for both the battery housing and the vehicle rocker. The main requirements for the divided rocker include providing high stiffness to the vehicle body, withstanding and transferring crash forces, and protecting the battery against deformation during a side crash event. There should also be an adequate mounting surface for the battery lid, and battery floor towards the battery-sided part of the divided rocker.

Another requirement is the ability to position, attach and detach the battery housing during the assembly and repair process. Therefore, the battery housing cannot be permanently bonded or glued to the vehicle body. To ensure detachability, for example, M10 bolts and nuts along the length of the vehicle rocker are used [21]. Deriving from this requirement, a boundary condition is defined that the battery housing must be attached from below using bolts along the length of the divided rocker. Hereby the location of the battery lid attachment point must be kept in mind so that the position of the bolts does not interfere with the battery housing lid. In order to have tool access at the attachment locations for the two halves of the divided rocker, holes of approximately 30 mm in diameter are needed. As the proposed designs should be comparable to each other, the division planes must have the same height for the battery structures. Therefore, the shape of the division plane should provide flat surfaces and location for positioning, attachment of battery lid, bolting, tool access and force transfer. Keeping these functional requirements in view, several possible division planes for the divided rocker are shown in Figure 2.

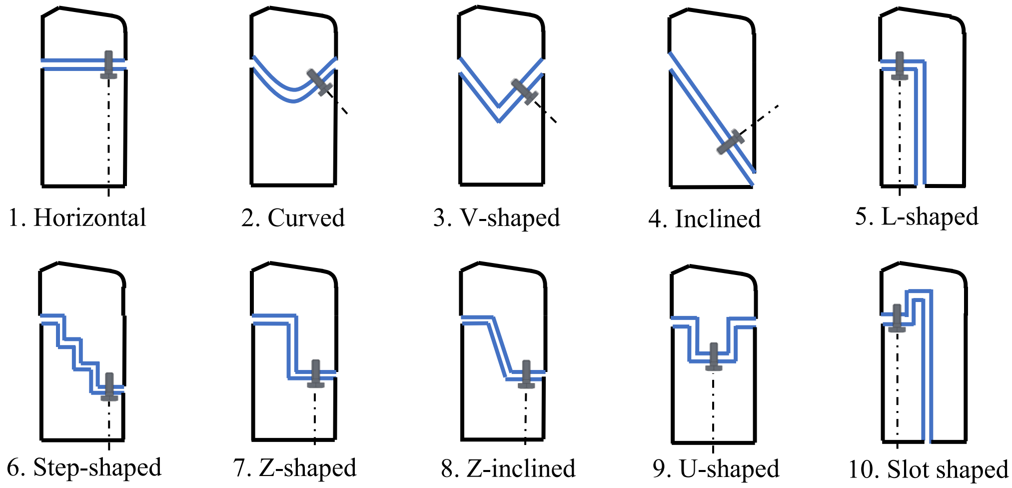


**Figure 2.** Division plane concepts for a divided vehicle rocker

Although these division planes partially fulfil the basic boundary conditions and design requirements, not all of them are equally suitable for manufacturing and assembly. Compared to each other, they differ regarding design complexity and additional functionality. For example, the horizontal division plane (1) is simple to manufacture and provides tool access from below. However, the curved (2) and V-shaped (3) division planes do not provide tool access from below and are also complex to manufacture due to curved and inclined surfaces. These division planes also form a double fit during assembly that might over-constrain the structure, taking both vehicle sides into account. The U-shaped (9) and the slot-shaped (10) division planes also have a double-fit design which would need tighter tolerances.

Similarly, the inclined (4) division plane is complex to manufacture due to the inclined shape and does not provide tool access from below. Moreover, the bolts in curved (2), V-shaped (3), and inclined (4) division planes would have shear stress in addition to axial stress, which should be avoided. The location of the bolts in L-shaped (5) and slot shaped (10) division planes is immediately adjacent to the attachment point for the battery housing lid. This location for the bolts not only needs tool access holes through multiple ribs adjacent to the battery but can also introduce immediate stress into the battery lid during the mounting process. Due to multiple small horizontal and vertical surfaces, the step-shaped (6) division plane is not only complex to manufacture but also has less surface area available for bolting. Both the Z-shaped (7) and Z-inclined (8) division planes provide vertical tool access from below. Here the bolts are not positioned on the same surface as the battery housing lid and therefore do not interfere during assembly. Additionally, these two-division planes are rather easy to manufacture. Furthermore, the vertical surface supports the positioning of the battery and therefore, can be advantageous in a side crash scenario [19].

After comparing the division planes based on their design complexity, surfaces available for positioning and lateral support during a crash, bolting location and direction, and tool access direction and distance, it is evident that some division planes fulfil the requirements better than others. Therefore, out of ten division plane concepts, three suitable division planes are selected and further investigated. The first initial design of these three division planes with internal chambers and bolts that can be accessed from below during the assembly process is shown in Figure 3.

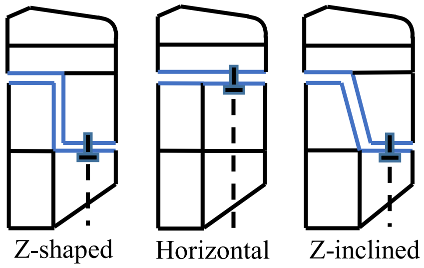


**Figure 3.** Modelled divided rocker division planes

In comparison, the horizontal division plane has relatively longer tool travel, whereas the tool travel in the Z-shaped and Z-inclined division planes is half the tool travel compared to the horizontal division plane. Therefore, the horizontal division plane needs more holes in the internal ribs to access the bolts, which might weaken the structure.

### Side Pole Component Level Crash Test Setup

The crash test setup for LS-DYNA based solver is shown in Figure 4. The crash test parameters are set up according to Euro NCAP side pole crash test [22]. The general setup on a component level is similar to the setup described in [18], [19]. The length, width and height of the divided rocker are similar to that of the reference vehicle rocker [20]. Bolted connections are defined between the two parts of the divided rocker along the length of the divided rocker. Several cross-members are modelled according to the positioning of the seat cross-members and the battery cross-members, similar to [19]. Solid elements are meshed to represent the weld connections between these cross-members and the divided rocker. At the other end, a supporting beam is modelled and attached to the cross-members.

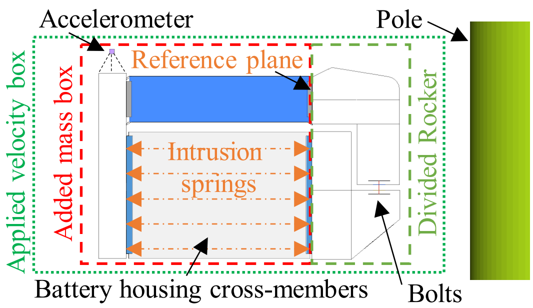


**Figure 4.** Side pole crash test setup

As a joining mechanism, several holes at the bolting location shown in Figure 4 are made along the length of the rocker for M10 bolts similar to [21]. For easy tool access from the bottom in the z-direction, multiple larger holes are made along the dotted lines, as shown in Figure 3. The components are then meshed in HyperMesh using shell elements. The vehicle rocker is divided into individual sections to vary the geometrical parameters later for parametric variations. The key dimensions of the modelled simulation setup are shown in Table 2.

**Table 2.** Key dimensions of setup components

| | |
|---|---|
| Diameter of pole | 254 mm |
| Length of the rocker | 1746 mm |
| Width of the rocker | 90 mm |
| Height of cross-members | 75 mm |
| Height of battery housing | 140 mm |
| Bolt hole diameter | 15 mm |
| Tool access hole diameter | 30 mm |
| Distance between holes | 150 mm |
| Element size | 5 mm |

The vehicle sided divided rocker and the seat cross members represent the supporting structure from the vehicle body, while the supporting structure of the battery housing consists of the battery sided cross members and the battery sided divided rocker on this component level test setup. The supporting beam together with the cross-members, resemble a simplified clamping structure. This simplified setup takes neither both vehicle sides nor the adjacent vehicle and battery structures such as reinforcing sheets, the vehicle side panel or the battery housing lid and floor into account.

In a side crash on a full vehicle level, the lateral load is usually distributed between additional components such as a-/b-/c- pillar roof cross members, dashboard cross members, rear long member, outer rocker, and door assembly [23]. On this component level setup, however, the load is distributed directly from the pole to the divided rocker and then to the seat and battery cross-members. Therefore, to approximate similar behaviour, the deformation of the given divided rocker concept on a full vehicle level is studied and used as the basis for the component level test setup. The aim of the test setup on a component level is to approximate similar structural deformation and rotation of the components compared to a full vehicle level test in [18], [19] through iterations. Taking into account the overall deformation of the vehicle rocker during a crash, a combined mass of 350 kg is added to the clamping structure to approximate the deformation of the rocker on a component level to the given deformation from the full vehicle test. Approximately 40% of the total added mass is located at the accelerometer point, while the remaining mass is distributed among the cross-members. The described distribution of mass was chosen to resemble the influences of the vehicle center of gravity and, therefore vehicular rotation, which would occur on a full vehicle level [19]. The rigid pole collides with the divided rocker in between the cross-members with a velocity of 32 km/h at a 75-degree angle, according to Euro NCAP side pole crash test [22].

Similar to state of the art, aluminum is used as a material for the vehicle rocker and cross members [21]. The divided rocker has a mass of 19 kg with material thicknesses assigned to different sections of the cross-section of the rocker ranging between 2.5 mm to 4.5 mm. For the battery cells in a battery electric vehicle, the deformation process during a side pole crash is the most critical in the vehicle's lateral direction due to the position of the battery cells relative to the vehicle structure [13]. Also, the maximum values of intrusion are more critical for the battery cells than the average values. Therefore, for this study, the maximum intrusion, maximum acceleration, and maximum force are measured along the lateral direction (y-direction). In total, ten intrusion springs are implemented to measure the structural deformation as a change in the length of the individual springs. The overall intrusion is determined as the maximum change of length along the y-direction in relation to the position of the reference plane shown in Figure 4. Acceleration is also measured as the maximum value along the y-direction. It is taken at the accelerometer point (as shown in Figure 4), where battery modules are typically positioned in a battery electric vehicle. Similarly, the maximum contact pole force which is equivalent to the maximum total force acting on the structure of the divided rocker is measured in the y direction. Finally, energy absorption is measured as the maximum total amount of energy absorbed by the divided rocker. An isometric view of the component level crash test setup is shown in Figure 5.

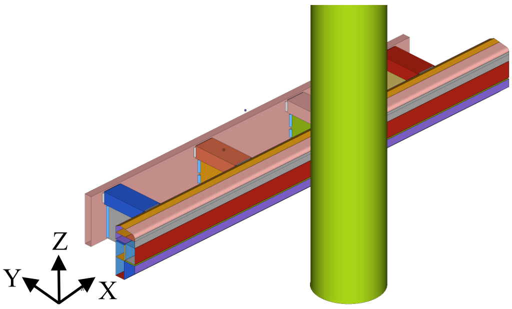


**Figure 5.** Isometric view of crash test setup

### Deformation Behaviour

Figure 6 shows the deformation behaviour of the Z-shaped division plane. At the beginning of the simulation (0 s), the whole structure is assigned an initial velocity of 32 km/h. The divided rocker collides with the pole at approximately 0.01 s, deforms plastically, and absorbs kinetic energy. As shown in Figure 7, the maximum deformation is reached at 0.015 s, after which the total deformation decreases. For the Z-shaped and Z-inclined division planes, the maximum deformation occurs at the middle height of the battery frame due to the bolting position. The same behaviour is visible for the horizontal division plane at the top of the battery frame due to the different bolting positions.

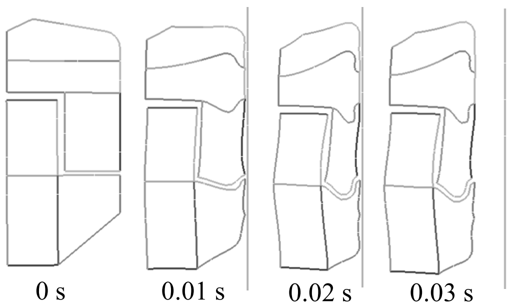


**Figure 6.** Deformation of z-division plane

As shown in Figure 7, the maximum intrusion for the Z-shaped division plane is 19.54 mm, while the maximum absorbed energy is 11.12 kJ. The maximum force and acceleration values, as shown in Figure 7, are relatively high compared to a full vehicle level side pole crash test. As mentioned earlier, this can be attributed to a number of factors.

First, the absence of surrounding vehicle structures such as b-pillar, door assembly structure, reinforcing sheets and the vehicle side panel present on a full vehicle level, and would also absorb energy along with the rocker during a side crash. Another reason for such high acceleration value can be the overall stiffness of the clamping structure that also has a significant effect on the bending behaviour and might be stiffer than the actual surrounding vehicle body structure. In the context of this paper, however, the magnitude of these values is used only as a reference for comparison between the different division planes regarding the parametric analysis. Here the resulting difference in crash performance is of higher significance than the actual nominal values.

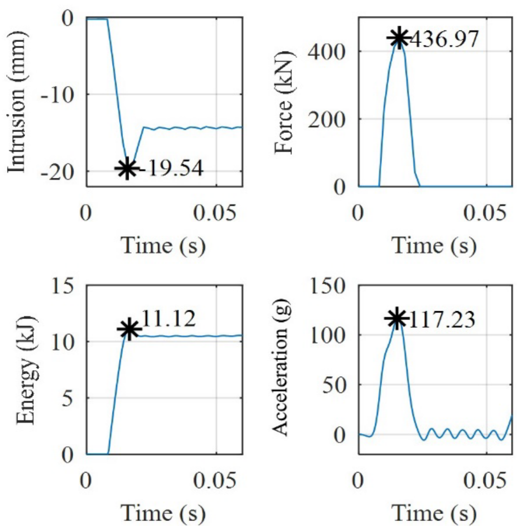


**Figure 7.** Crash performance of Z-shaped division plane

## PARAMETRIC ANALYSIS

To create parametric variations, several design limitations are defined. For example, all variations must remain within the pre-defined space for the divided rocker. The variations must not decrease the space available for the battery. Also, the variations must have the same choice of material, bolting location, and a similar assembly process. Each parameter is therefore varied within a defined range, and the resulting influence on the crash performance is observed. The goal of the parametric analysis is to identify the resulting effects from changing parameters and derive possible improvements for the crash performance based on the studied effects while maintaining a lightweight design. Figure 8 illustrates the investigated parameters for the three division planes.

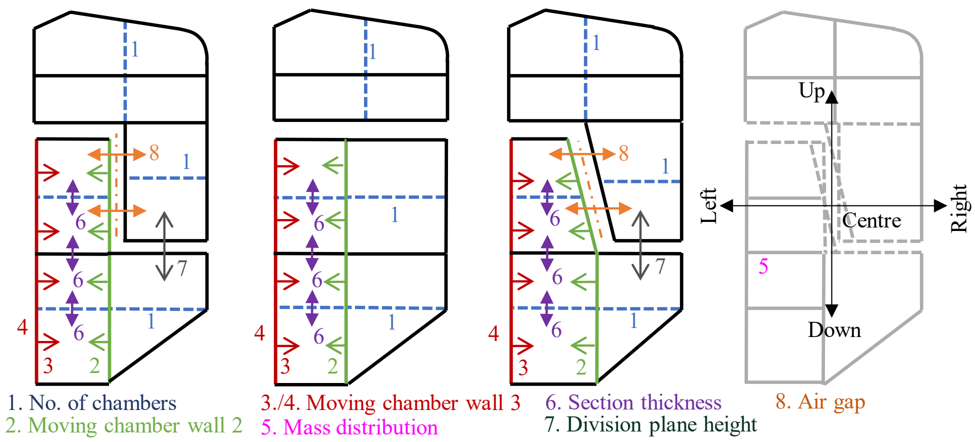


**Figure 8.** Schematic of parameters considered for parametric analysis

The initial design has six internal chambers, as shown earlier in Figure 3. To study the effect of number of chambers on crash performance, the total number of chambers is changed in four variations from 6 to 12. Based on the measured intrusion, it is observed that in this scenario, a 10-chamber design performs better on a component level and is therefore considered for the next step, as shown in Table 3. The second studied parameter is the chamber width, which is varied in two different ways. First, the right chamber wall (indexed with "2" in Figure 8) is moved towards the left while maintaining the positioning of the opposite chamber wall. Secondly, the left chamber wall (indexed with "3" in Figure 8) is moved towards the right while keeping the opposite one constant. Both scenarios lead to chamber width variations between 25 mm to 40 mm in increments of 5 mm. While changing the chamber width by moving the chamber wall “2” towards the left, additional air gaps can be created in favour of foreseeing tolerances.

**Table 3.** Overview of the parametric analysis

| Step | Mass (kg) | Number of chambers | Chamber width (mm) | Space created for battery modules (mm) | Mass distribution | Sectional thickness (mm) | Division plane height (mm) | Air gap (mm) |
|---|---|---|---|---|---|---|---|---|
| 1. | 19 | 6-12 | 40 | 0 | - | 2.5 to 3.5 | 0 | 2 |
| 2. | 18.5-19 | 10 | 25-40 | 0 | - | 2.5 | 0 | 2 |
| 3. | 17.9-19 | 12 | 25-40 | 0-15 | - | 2.5 | 0 | 2 |
| 4. | 17.9-19 | 10 | 25-40 | 0-15 | - | 2.5 | 0 | 2 |
| 5. | 17.9 | 10 | 25 | 15 | varied | 2.7 to 4.2 | 0 | 2 |
| 6. | 17.9 | 10 | 25 | 15 | - | 2.5-3.5 | 0 | 2 |
| 7. | 17.5 to 18.3 | 12 | 25 | 15 | - | 2.5 | -30, 0, +30 | 2 |
| 8. | 17.6 to 17.9 | 10 | 25 | 15 | - | 2.5 | 0 | 0-8 |

While changing the chamber width by moving the chamber wall “3” towards the right, additional package space is created for the battery modules. The second variation is performed for both a 10-chamber and a 12-chamber design to study the interdependence of the chamber width on the number of chambers, as shown in step 2 and step 3 of Table 3. Based on the results from the first four steps, a 10-chamber design having 25 mm chamber width and 15 mm additional package space for the battery modules shows lower intrusion while also having less mass. Therefore, this design is chosen for the next steps of variation.

The fifth variation is the distribution of the mass within the rocker structure. For this step, the material thickness is varied within the limit of 2.7 mm and 4.2 mm. The average difference in thickness between cross-sections for each variation in this step is 1 mm. In this way, the mass of the divided rocker is shifted to different locations, such as towards left, right, up, down, and centre.

Additionally, the mass is also shifted across horizontal and vertical cross-sections within the divided rocker. To observe the influence of individual section thicknesses regarding the inner chambers in the lower part of the divided rocker, the material thickness is varied between 2.5 mm and 3.5 mm in the sixth variation, as shown in Figure 8. In the seventh variation, the influence of the division plane height on crash performance is investigated. As any change in the height of the horizontal division plane would also change the height of the battery, this variation is only studied for the Z-shaped and Z-inclined division planes.

Moreover, for this variation, a 10-chamber design is not suitable as moving the division plane 30 mm up or down would change the size of chambers towards the right of the divided rocker, resulting in unequal chambers above and below the division plane. Therefore, this variation is performed on a 12-chamber design since in this design, the division plane movement would still result in equal chamber sizes in all variations within this step. Similarly, the air gap between the vertical surfaces in the Z-shaped and Z-inclined division planes is varied between 0 mm to 8 mm in increments of 2 mm. Again, the influence of this parameter cannot be studied for the horizontal division plane since it lacks a vertical supporting surface between the two parts of the divided rocker. All geometric variations shown in Figure 8 and the steps given in Table 3 are performed at 32 km/h with 350 kg mass added to the structure.

### Intrusion

Without the consideration of other parameters, in this component level test, the measured maximum intrusion towards the battery is the lowest for a 10-chamber design, as shown in Figure 9. Moving the chamber wall towards the right and creating narrower chambers results in lower intrusion for all three division planes. This trend is consistent for both the 10-chamber and the 12-chamber designs as evident from Figure 9. As the chamber wall moves towards the right, the area of the rocker and, consequently the moment of inertia decreases. The resulting deformation is higher in step 3 and 4. However, since it is always measured in relation to the reference plane shown in Figure 4, despite higher total deformation, the measured maximum intrusion shown in Figure 9 is lower. In this way, additional package space is created for the battery modules while also reducing the measured intrusion. Out of the seven variations performed for the mass distribution within the divided rocker, the least intrusion is observed when the mass is distributed upwards in the Z-shaped and Z-inclined division planes.

As evident from Figure 9, changing the section thicknesses and the division plane height do not show any significant changes in the maximum intrusion. Also, changing the air gap between the vertical surfaces of the Z-shaped and Z-inclined division planes has a small and inconsistent influence on intrusion. Between the three division planes, the Z-inclined division plane has the highest intrusions, while the Z-shaped and the horizontal division planes have comparable maximum intrusion values when the parameters are assigned properly. The measured intrusion results indicate that the change in parameters within the division planes has a more significant influence on the crash performance as compared to the choice of division planes itself. Among these parameters, the chamber wall movement is the most noticeable parameter, as it decreases maximum intrusions while also creating additional space for the battery modules.

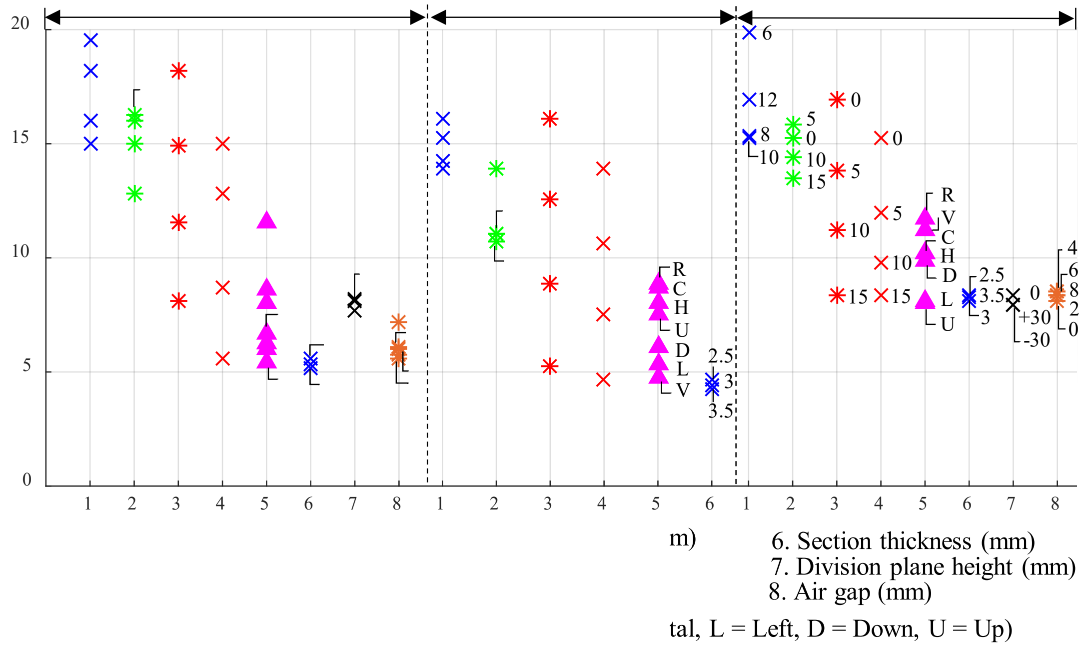


**Figure 9.** Influence on maximum intrusion for three division planes

## Force

The number of chambers has a noticeable but incoherent influence on the maximum force acting on the divided rocker. The results for the maximum force values for the three division planes are shown in Figure 10. In step 1, a 6-chamber design results in less force in all three division planes. However, as the number of chambers increases, the maximum force does not increase in a linear and coherent way. This indicates that in addition to the number of chambers, the influence might also depend on the location of these chambers within the divided rocker. On the other hand, the movement of the chamber walls has a direct and coherent influence on the force. As the chambers walls are moved and the chamber width is decreased, the maximum force acting on the structure is also decreased. When chamber wall 3 is moved towards the right, the overall deformation and intrusion are higher due to the decrease in total area and the moment of inertia of the divided rocker. Due to the increased total deformation, the maximum force on the structure decreases. This influence is consistent regardless of the number of chambers, as shown in step 3 and step 4 of Figure 10.

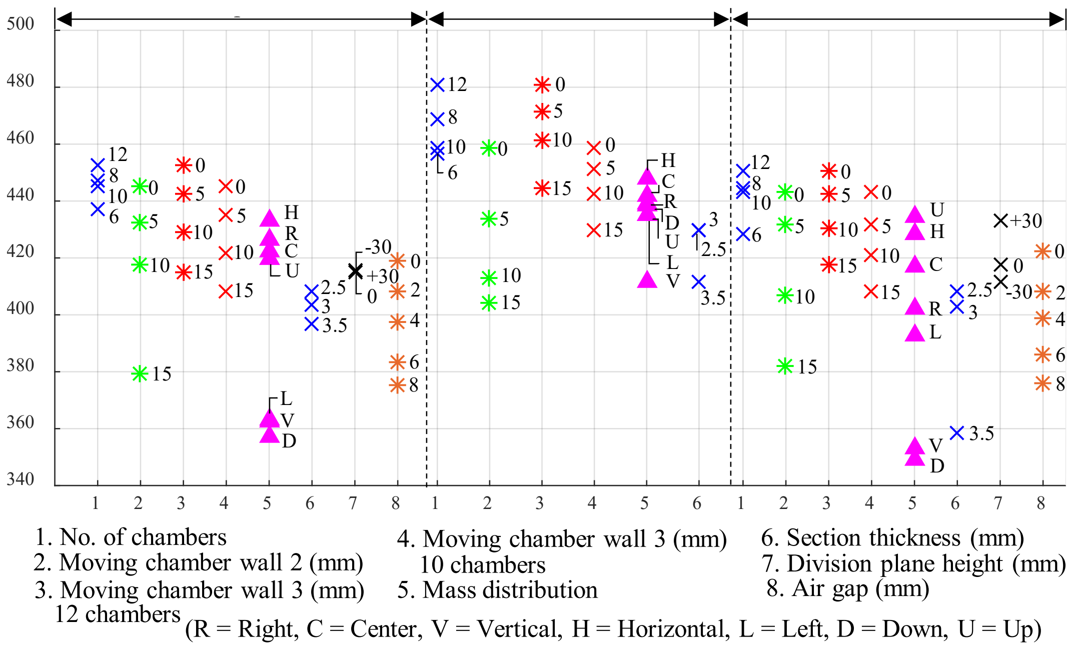


**Figure 10:** Influence on maximum force for three division planes

The measured force is higher when the structure is stiffer, and the mass is distributed in the direction of the impact. In addition, the mass shifted towards the left and in the vertical direction has lower maximum force values, while mass concentrated in the horizontal direction has relatively higher maximum force values for all three division planes. With respect to the air gap, there is a notable and consistent influence on force, with the larger air gap resulting in lower forces.

For this variation, the maximum force is the highest when there is no air gap present. In contrast to the trends observed for intrusion, the horizontal division plane has higher force values for all the parametric variations as compared to the Z-shaped and the Z-inclined division planes. This is due to the impact energies being identical.

### Energy

For the three studied division planes, the maximum energy absorption does not vary with the number of chambers with a consistent pattern. However, for the variation of the chamber wall movement, the influence on maximum energy absorption is consistent across all three division planes. Generally, as the chamber walls of the lower rocker are moved and narrower chambers are created towards the left, the maximum energy absorption is increased. The reason, again, is the increase in overall deformation in the structure and the creation of larger deformable chambers towards the right of the structure that absorb energy. The equivalent variation also results in a reduction of the measured intrusion and force. The influence of the distribution of the mass within the divided rocker is consistent with the maximum energy absorption.

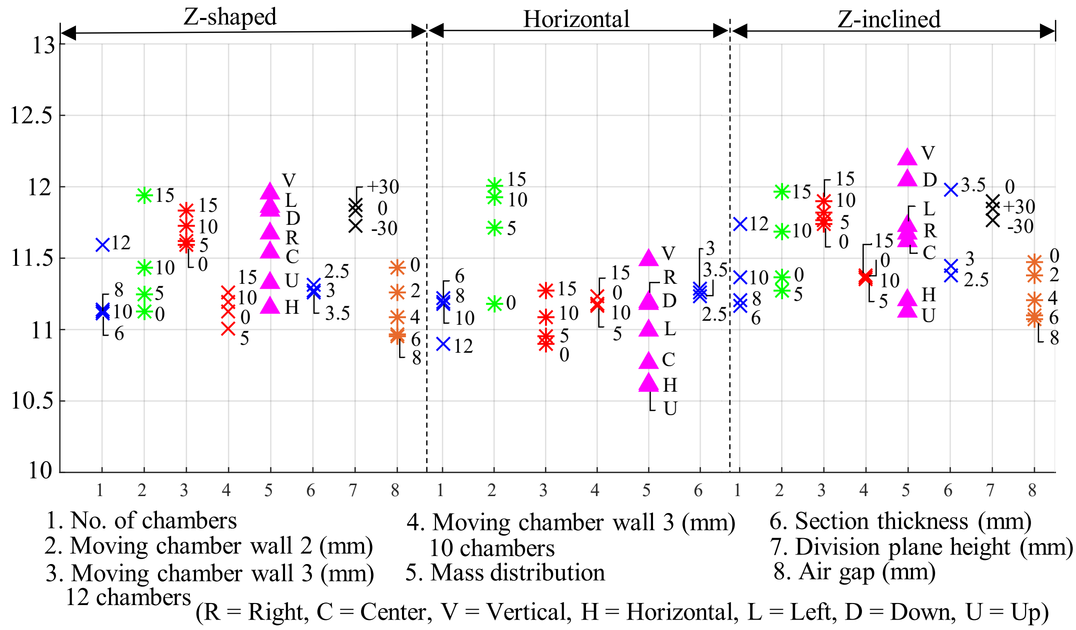


**Figure 11.** Influence on maximum energy absorption for three division planes

The highest energy absorption occurs when the mass is distributed in the vertical direction. In this way, lower material thicknesses are assigned to the horizontal cross-sections which are along the direction of the impact, thereby increasing the plastic deformation and the maximum energy absorption. As seen in Figure 11, a clear pattern regarding energy absorption is visible for the variation of the air gap in the Z-shaped and the Z-inclined division planes. The energy absorbed is the highest, like force, when there is no air gap present between the vertical surfaces of the division planes. As the gap increases, the energy absorption decreases, and the lowest energy absorption occurs at a gap of 8 mm for both division planes.

## RESULTS AND DISCUSSION

The results achieved at the component level will be discussed in the following section. Analyzing the crash performance regarding the investigated criteria (intrusion, force, and energy absorption) suggests that there are contradicting trends regarding the crash performance except for the influence of the chamber wall movement. For example, a larger air gap results in lower maximum forces and maximum accelerations but also has less maximum energy absorption.

However, parameters like the position and the movement of the chamber walls are beneficial from the perspective of all three crash performance criteria. Using narrower chambers towards the left (by moving chamber wall 3 in the lower part of the rocker) results in lower maximum intrusions, lower maximum forces, and higher energy absorption in all three division planes. Therefore, it is the most notable, significant, and consistent trend that also has the potential to improve the crash performance across the addressed criteria. Another benefit is the reduction of mass and added space for the battery modules when the chamber walls are moved towards the right. This trend of decreasing intrusion values using narrower chambers towards the left is consistent with the trend observed in [19].

Another influential trend is the number of chambers in the internal geometry of the divided rocker. For the Z-shaped and Z-inclined division planes, the lowest number of chambers have the highest intrusions. This trend was also observed in the results from [18], [19] where an increase in number of chambers by the addition of internal ribs resulted in lower intrusion values for Z-shaped division plane.

Between the three division planes, for this setup on a component level, the Z-shaped division plane performs better than the Z-inclined division plane, while the horizontal division plane has comparatively slightly lower intrusion values than the other two division planes. However, the horizontal division plane consistently has higher values of maximum force, and lower values of maximum energy absorption. The differences in crash performance are neither significant nor consistent between the three division planes as compared to the differences due to the parametric variations within each division plane.

Therefore, the selection of one division plane over the other should consider crash performance as well as design criteria for the intended application. The Z-inclined division plane has several design concerns. The inclined surface of the Z-inclined division plane may result in a larger vertical component of the force being applied to the battery during the crash event. This inclined surface may exert additional stress on the bolts and might push the battery out of the vehicle structure. Therefore, this aspect of the design of the Z-inclined division plane needs to be further investigated. Moreover, tolerances and manufacturability due to the inclined shape of the division plane also need to be considered.

Similarly, the horizontal division plane lacks a vertical surface to support the battery housing on both sides of the vehicle. The upper part of the divided rocker for the horizontal division plane is only about 35% of the total rocker area. This not only restricts the design possibilities [19] but also limits the attachment points of vehicle body structures. Concerns about the structural stiffness and the ability of the rocker to withstand structural load during the absence of the lower battery-sided rocker are raised and need to be further investigated. The horizontal design might create stress around the battery lid mounting location as the bolts are in the same plane as the battery lid [19]. This should be addressed in further investigations.

Due to the potentially higher surface area of the division plane, the Z-shaped variant has lower section thicknesses for the same structural mass and therefore has slightly higher deformation values on a component level compared to the horizontal division plane. However, from a design perspective, the Z-shaped division plane avoids the aforementioned restrictions, especially regarding the vehicle sided attachment possibilities and therefore, provides the largest design freedom [19]. Taking both sides of the vehicle into account, the Z-shaped and Z-inclined division planes might need tolerance consideration to avoid double fit during assembly. Such tolerance considerations were not further highlighted in this paper, based on the investigations on a component level.

The studied parameters highlight the behaviour of the divided vehicle rocker on a component level. Since vehicle-sided structures are not taken into account, the final choice of design and dimensioning of the divided rocker must be done on a full vehicle level. However, the investigated influences on a component level can be considered as a starting point. In this regard, the effect of the chamber width is the most significant.

## CONCLUSIONS

In this paper, a divided rocker concept for a functionally integrated battery housing was taken from an existing study [19], and design possibilities for the division plane were created and studied. After evaluating the division planes based on design, positioning, bolting, and tool access, three division planes (Z-shaped, horizontal, and Z-inclined) were selected and further investigated. A side pole crash test was set up on a component level in a LS-DYNA based solver. The crash performance of the three division planes was studied. The division planes showed similar deformation behaviour. A parametric analysis of the three division planes for the divided rocker was performed. The parameters varied for the analysis included the number of chambers, the width of the chambers, the distribution of the mass within the rocker structure, the material thicknesses of the individual sections, the height of the division planes, and the air gap between the vertical surfaces of the division planes.

Based on the results, several trends regarding the crash performance were identified, and the influences on intrusion, force, and energy absorption were investigated. From the results, it was concluded that the chamber width has the most significant influence on intrusion, force, and energy absorption. Designing smaller, stiffened chambers towards the battery (left) in the lower part of the divided rocker and bigger chambers towards the right had an overall positive effect on the crash performance.

The parameters investigated and influences observed in this paper are limited to the crash performance resulting from a component level side pole crash test. The influence and attachment of different components such as b-pillar and door assembly present on a full vehicle level were not considered. The deformation behaviour for the studied division planes might differ on a full vehicle level due to the interaction with additional components, which could influence the deformation behaviour. Therefore, the final design and dimensioning of the divided rocker should be further explored on a full vehicle level.

## ACKNOWLEDGEMENT

I am grateful for the continued support of Mr. Christopher Krüger and Prof. Dr.-Ing. Peter Urban during the entire research process. I am also thankful to DAAD for funding this research at IKA Institute of RWTH Aachen.

## REFERENCES

[1] European Commission, "EU climate action and the European Green Deal," 2021. [Online]. Available: https://ec.europa.eu/clima/policies/eu-climate-action_en. [Accessed: July 21, 2021]

[2] The White House FACT SHEET, "President Biden Sets 2030 Greenhouse Gas Pollution Reduction Target Aimed at Creating Good-Paying Union Jobs and Securing U.S. Leadership on Clean Energy Technologies," 2021. [Online]. Available: https://www.whitehouse.gov/briefing-room. [Accessed: Apr. 28, 2021]

[3] C. Julian, “Why the automotive future is electric?,” 2021. [Online]. Available: https://www.mckinsey.com/industries/-automotive-and-assembly/our-insights/why-the-automotive-future-is-electric. [Accessed: Sept. 2, 2021]
[4] J. Deng, C. Bae, A. Denlinger, and T. Miller, “Electric vehicles batteries: Requirements and challenges, ” *Joule*, vol. 4, issue 3, pp. 509-515, 2020
[5] M. Schäffer, M. Münster, M. Sturm, and Freidrich, “Development of an optimized side crash concept for the battery-electric vehicle concept urban modular vehicle,” In Proc. 14th LS-DYNA Forum, Bamberg, Deutschland, 2016.
[6] P. Victor Chombo, Y. Laoonual, and S. Wongwises, “Lessons from the electric vehicle crashworthiness leading to battery fire,” *Energies*, vol. 14, p. 4802, 2021
[7] EV Database, 2021. [Online]. Available: https://ev-database.org/. [Accessed: May 24, 2021]
[8] The battery: Sophisticated thermal management, 800-volt system voltage, Porsche Newsroom, 2021 [Online]. Available: https://newsroom.porsche.com/en/products/taycan/battery-18557.html; [Accessed: June 5, 2021].
[9] TÜV SÜD, New Mandatory Safety Testing Requirements for electric vehicle batteries under R100, 2019. [Online]. Available: https://www.tuvsud.com/en/resource-centre/white-papers/new-mandatory-safety-testing-requirements-for-electric-vehicle-batteries-under-r100. [Accessed: Apr. 16, 2021]
[10] Inficon. Leak Testing of Components, Battery Packs for EVs/HEVs. Inficon, Bad Regaz, 2019. [Online]. Available: https:// www. infic on.com/ v1/ attachment/ Leak- Testi ng- Batte ry- Packs/ mial0 0en_ 04(1903). Pdf. [Accessed: Nov. 29, 2022]
[11] UN ECE R 100-2. Regulation No 100 of the United Nations Economic Commission for Europe (UNECE) - Uniform provisions concerning the approval of vehicles with regard to specific requirements for the electric powertrain [2015/505]. United Nations Economic Commission for Europe, 2015
[12] Safety Companion 2021. Carhs GmbH, Germany; 2021
[13] G. Tandon, “Integrated battery and occupant protection body-in- white concept using tailored blanks,” *Batteriesysteme im Karosseriebau*, Bad Nauheim, 2020.
[14] M. Wisch, J. Ott, R. Thompson, Y. Léost, M. Abert, and J. Yao, “Recommendations and Guidelines for Battery Crash Safety and Post-Crash Safe Handling, Transport and Research and Innovation Monitoring and Information System (TRIMIS),” 2014
[15] H. Löbberding, S. Wessel, C. Offermanns, M. Kehrer, J. Rother *et al.*, “From cell to battery system in bevs: analysis of system packing efficiency and cell types,” *World Electric Vehicle Journal*, vol.11, no. 4, p. 77, 2020
[16] R. Schmerler, T. Gebken, S. Kalka, and T. Reincke, “Multi-functional battery housing for electric vehicles,” *Lightweight Design Worldwide*, vol. 10, Berlin, Germany, vol. 10, pp. 26-31, 2017
[17] A. Bala, M. Chaitanya Kamaraju, “Design and optimization of battery housing in electric cars,” M. S. thesis, Chalmers University of Technology, Gothenburg, Sweden, 2020
[18] T. Schmolke, C. Krüger, D. Merdivan, S. Spohr. “Entwicklung einer gewichtsoptimierten Batteriegehäusestruktur für Volumenfahrzeuge,” In Proc. FAT-Schriftenreihe p. 352, 2021
[19] C. Krüger, S. Spohr, D. Merdivan *et al.*, “Avoiding structural redundancies between the vehicle body and the battery housing based on a functional integration approach,” *Automotive and Engine Technology*, vol.7, no. 7, pp. 197–208, 2022
[20] J. Meschke, J. Tölle, and L. Berger, “Multimaterialkonzept für ein Elektrofahrzeug,” *ATZ-Automobiltechnische Zeitschrift*, vol. 119, pp. 48–53, 2017
[21] I. Lüken, N. Tenneberg, Volkswagen ID.3, Body-in-white structure in interaction with high-voltage battery housing (HVBH) Volkswagen AG, Germany, *Aachener Karosserietage*, Aachen, Germany, 2019.
[22] European New Car Assessment Programme. Obilique Pole Side Impact. Testing Protocol Euro NCAP, Brüssel, 2019. [Online]. Available: https:// cdn. Euroncap. com/ media/ 55860/ euro- ncap- pole- proto col- obliq ue- impactv711.pdf. [Accessed: Nov. 29, 2022]
[23] L. Eckstein, *Structural design of vehicles*, Aachen: Institut für Kraftfahrzeuge, RWTH, 2013